מכון ויצמן למדע
WEIZMANN INSTITUTE OF SCIENCE

Thesis for a degree

Master of Science

By

Chen Ken Shalem

חיבור לשם קבלת תואר

מוסמך מדעים

מאת

חן שלם

R&D of a novel gas electron multiplier – the THGEM

חקר ופיתוח של מכפל אלקטרונים גזי חדיש

Advised by
Prof. Amos Breskin
Dr. Rachel Chechik

בהדרכת
פרופ. עמוס ברסקין
ד"ר רחל צ'צ'יק

March 2005

מאי 2005

Submitted to the Scientific Council of the Weizmann Institute of Science
Rehovot, Israel

Abstract

The operation mechanism and properties of Thick GEM-like (THGEM) gaseous electron multipliers, operated at atmospheric and low pressure, are presented. They are made of standard printed-circuit board, perforated with sub-millimeter diameter holes, etched at their rims. Gas multiplication factors of 10^5 and 10^7 at low (1 Torr) and atmospheric pressure respectively were obtained. Fast pulses in the few nanosecond rise-time scale were reached in single and cascaded double-THGEM elements, in standard gas mixtures with single photoelectrons. Energy resolution of 20% FWHM was recorded with 5.9 keV X-rays at a gain of 10^5. High single-electron detection efficiency is obtained in photon detectors combining THGEMs and semitransparent UV-sensitive CsI photocathodes or reflective ones deposited on the top THGEM face; the latter benefits of a reduced sensitivity to ionizing background radiation. Stable operation was recorded with photoelectron fluxes up to the MHz/mm^2 scale. Some potential applications of these simple and robust multipliers are discussed.

Acknowledgments

It is my pleasure to thank all those who helped me during the experimental and theoretical work of my master thesis at the Weizmann Institute of Science.

In particular I would like to extend special thanks:

To **Dr. Rachel Chechik** who was the originator of the THGEM project, for her conceptual and practical help during the work and especially for her delicate assist in the writing effort.

To **Prof. Amos Berskin** for guiding the project using his huge knowledge in the field of radiation detection, and for his personal help regarding my future plans.

To **Moshe Klin** who brought the light to the laboratory through his electronics skills and through his warm personality.

To **Nachum Zwang** for his technical help and moreover for his speciel encouragements.

To **Keren Michaeli, Nir Ben-Haim, Yonathan Schwarzkopf, Marco Cortesi** and **Alexey Lyashenko** for taking part in measurements and theoretical calculations.

To my **class mates**, and especially **Itai Afek** and **Ido Mizrahi**, for their help during the first year courses.

It is due to your help that the work was finally carried out.

Contents

1. Introduction

In this work we present a novel concept and tool for the detection of charged particles and photons: the thick gas electron multiplier (THGEM) [1, 2 and 3]. It is a robust, simple to manufacture, high-gain gaseous electron multiplier. Its operation is based on gas multiplication within small, sub-millimeter to millimeter diameter holes. The thesis work comprises on one hand conceptual design studies based on simulations of electric field distributions and of charge transport and multiplication in single and cascaded THGEMs; on the other hand it comprises detailed experimental investigations of the properties of the new multipliers over a broad range of gases and pressures. An accent was put on the application to the detection of single photons.

Gas avalanche multiplication within small holes is attractive because the avalanche-confinement in the hole strongly reduces photon-mediated secondary effects. In addition, hole-multiplication provides true pixilated radiation localization. Hole-based multiplication has been the subject of numerous studies in a large variety of applications. Among them: optical particle tracking by gas discharge in capillary plates and tubes [4]; Gamma radiation detection with small diameter lead-glass and other tube-like converters followed by charge multiplication within the "holes" [5,6]; proportional amplification in other structures like the Micro-Well [7] and the glass Capillary Plates (CP) [8,9] etc. More details are provided in paragraph 2.5.

The most attractive and extensively studied hole-multiplier is the Gas Electron Multiplier (GEM) [10], comprising 50-70-μm diameter holes chemically etched in a 50-μm thick metalized Kapton foil.

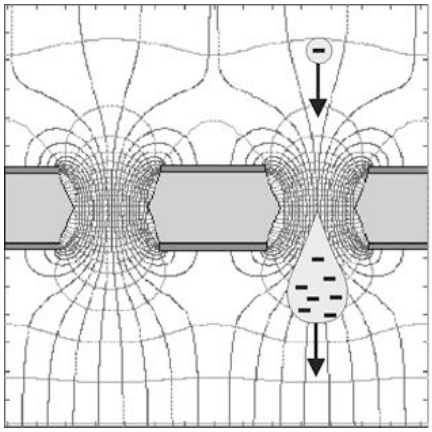

Figure 1: Schematic view of the operational principle of the standard GEM. Electrons follow the field lines and are focused into the holes, where an avalanche multiplication process takes place at the strong electric field there.

Its operation principle is based on electron multiplication inside gas medium; electron drift into the GEM holes, where due to a strong electric field (~80 kV/cm) they gain enough energy to ionize the gas molecule, which, as shown in figure 1, results in avalanche process. It operates in a large variety of gases, including noble-gas mixtures, providing a gain of ~10^4 in a single element and gains exceeding 10^6 in a cascade of 3-4 elements [11,12].

Our THGEM is actually a geometrically expanded version of the standard GEM, with all dimensions expended by about an order of magnitude. It is fabricated in standard printed-circuit board (PCB) technique; unlike the "optimized GEM" developed by Peskov et al.[13], our concept combines in addition to hole drilling in a PCB also chemical etching of the copper at the rim around each hole (Fig.2). The latter was found essential for reducing considerably discharges at the hole's rim, resulting in higher permissible voltages, better stability and higher gains.

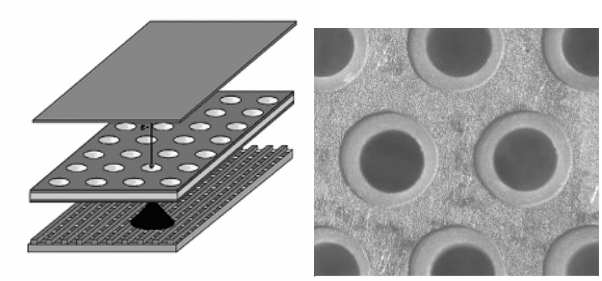

Figure 2: Left: a schematic view of the THGEM operation principle. Right: a photograph of a THGEM#9: 0.4 mm thickness, 0.3 mm hole diameter and 0.7 mm pitch. A rim of 0.1 mm is etched around the drilled holes.

Though the geometrical dimensions of the THGEM are expanded by large factors, most parameters governing its operation, e.g. operation voltage, electric fields, electron diffusion, etc. do not scale accordingly. Therefore, the optimization of the THGEM parameters required a broad systematic study. In the present thesis work, we have investigated a large variety of THGEM geometries over a broad pressure range (0.5-760 Torr); we will provide the optimal geometry in terms of hole diameter, hole spacing and electrode thickness, for different applications at atmospheric and low gas pressures.

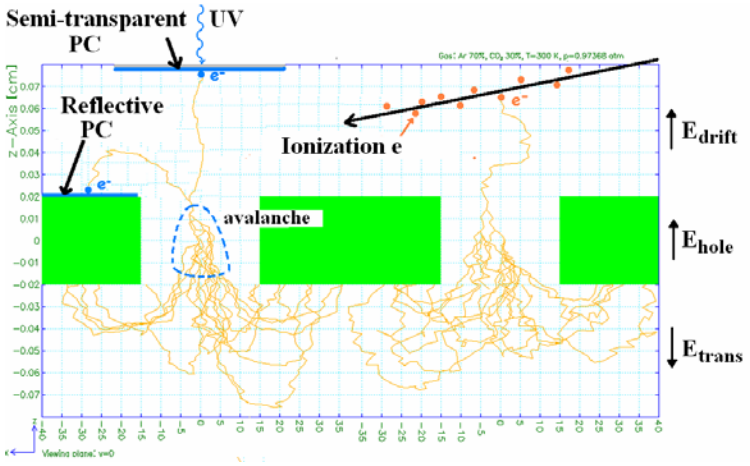

Figure 3: The operation principle of the THGEM demonstrated by GARFIELD [31] simulation at low THGEM gain (~30): electrons originating from gas ionization or from a semitransparent or reflective photocathode are focused into the holes, where they undergo avalanche multiplication. Depending on the size and direction of the field E_{trans}, avalanche electrons are further transferred to a readout electrode, to a second multiplier, or are collected at the THGEM bottom electrode as shown here with a reversed E_{trans}.

The THGEM operation principle, which is identical to that of a standard GEM, is shown in Fig.3. Upon application of a voltage difference across the THGEM, a strong dipole field E_{hole} is established within the holes. Electrons deposited by ionizing radiation in a conversion region above the THGEM, or produced on a solid radiation converter (e.g. a photocathode (PC)), are drifting towards the THGEM under the field E_{drift} and are focused into the THGEM holes by the strong electric field inside the holes. The PC can be a *semitransparent (ST)* one, placed above the THGEM, or a *reflective (Ref)* one, deposited on the THGEM top surface. With *Ref* PCs the most appropriate E_{drift} value is 0, as discussed below; with *ST* ones, a drift field of 0.1-1 kV/cm is required, according to the application. The electrons are multiplied within the holes under the high electric field (~25-50 kV/cm); depending on the size and direction of the field E_{trans}, a fraction of the resulting avalanche electrons are collected on the THGEM bottom electrode while the rest may be further transferred to a collecting anode or to a second, possibly similar, multiplier element. Each hole acts as an independent multiplier; the avalanche confinement within the holes has the advantage of reduced photon-mediated secondary effects; this leads to high-gain operation in a large variety of gases, including highly scintillating ones like pure CF_4.
Using a *Ref* PC deposited on the THGEM top face is particularly interesting: in this geometry the PC is totally concealed from avalanche-induced photons and therefore no photon-feedback effects (generally yielding unwanted secondary avalanches) are present. As the latter are a major performance-limiting mechanism of photon-imaging detectors, [14], their suppression is of advantage for conceiving high-efficiency detectors with sensitive PCs.
We shall present results demonstrating the role of each geometrical and operational parameter of the THGEM. The operation and properties of photon detectors with *ST* and *Ref* PCs and of soft x-ray detectors will be described.

The THGEM multiplier-detector has many applications in the field of particle physics, where moderate sub-millimeter localization resolution is sufficient. At atmospheric pressure it can be used for UV-photon detection and imaging of Cherenkov light, e.g. in Ring Imaging Cherenkov (RICH) detectors for particle identification [14] and for particle tracking, e.g. In Time Projection Chambers (TPC) [15]. As demonstrated in this work, the THGEM can also operate at very low gas pressures (below 1 Torr); possible applications are in detecting heavily ionizing particles and possibly, the detection of very low energy ions, discussed below.

2. The physics of gaseous detectors

2.1 Detection of charged particles and photons.

Charged particles and photons traveling inside a gas medium can interact with it in many ways. The most probable interaction generally used for detection is the electromagnetic interaction, which results in both excitation and ionization of the gas molecules. The energy required for creating an electron-ion pair depends on the gas type and is typically around 25-35 eV.

Photon interactions with the gas molecules depend on the photon energy. At low energy up to several keV, the dominant process is the photoelectric one. At the range over 10 keV Compton scattering takes over and at energies above MeV electron-positron pair production is the most probable process. The process of photoelectric absorption is the most common process in our experiments, encompassing either UV-photons or soft (5.9 keV) x-rays. In our experiments, x-rays were absorbed in gas resulting in its ionization by the emitted primary electrons; on the contrary, the UV photons interacted with a solid CsI photocathode, which requires only 5 eV to create a free electron, resulting in photoelectrons emitted into the gas medium.

The study of UV photon detectors, combining solid radiation converters with gaseous electron multipliers, has been a major research topic in our group for many years [16]. The quantum efficiency (QE) of solid photo-converters (photocathodes), which is the probability of electron emission per incoming photon, is an intrinsic property of the converter; it depends on the photocathode material, the status of its surface, and the photon wavelength. When operating in a gas environment, the QE is reduced by photoelectron backscattering on the gas molecules [17]. CsI is the most common UV photocathode [18]. In a recent work, a 2500A thick CsI photocathode deposited on a GEM surface, yielded a QE of 23% with 180nm UV photons [19].

X-ray interaction with the gas molecules is a quantum process involving one or more transitions in the atomic electron shells of the gas molecule components. The attenuation of the x-ray flux in the medium is a function of its energy and of the medium composition. Its absorption length in the medium is given by:

$$\lambda = \frac{1}{N\sigma}$$

Where N is the gas density and σ is the cross section for collisions.

Absorption of 5.9 keV x-ray photons, for example, in the Argon atomic shell (E_j) of 3.2 keV results in the emission of a primary photoelectron with an energy 5.9-3.2=2.7 keV. The photoelectron will have a range of about 100 microns at one atmosphere. The residual ionized and excited molecule can decay to its ground state mainly via two mechanisms:

1. Fluorescence: i.e. internal electron transition with photon emission E_j-E_i (from atomic level E_j to lower atomic level E_i). This secondary photon has an energy smaller than the ionization threshold and thus a very long mean-free-path for absorption; it can therefore escape the volume of the detector.

2. Radiation-less transitions (Auger effect): a rearrangement of the atomic electrons followed by the emission of a second electron of energy 3.2 keV.

In Argon for example, in 15% of the cases we have photon emission and in 85% of the cases: two electrons emission.

The passage of a charged particle in a medium result in a discrete number of primary ionizing collisions, which liberate primary election-ion pairs (n_p). Some ejected electrons can have enough energy to further ionize the medium, producing secondary electron-ion pairs; the total number of electron-ion pairs can be express by:

$$n_T = \frac{\Delta E}{W_i}$$

Where, ΔE is the energy-loss in the medium (e.g. gas volume), and W_i is the effective average energy to produce one pair.

In Ar/CO_2 (70:30), for example, 34 primary pairs will result in a total of 124 electrons-ion pairs [20]. The total charge created in the gas is either collected at the read out electrode (ionization chamber mode) or is multiplied in the gas, as discussed below, to yield detectable pulse-signals; the latter, proportional to the deposited energy, provide time and localization information.

2.2 Ion and electron transport inside gas media

When an electric field E is applied across the gas volume, a net movement of the ions along E direction is observed. This net movement is the outcome of collisions with the gas molecules and acceleration by the field E between successive collisions. The average velocity of this slow motion is called ion drift velocity w^+ and it is found to be linearly proportional to E/p; p being the gas pressure. The ion mobility is defined as

$$\mu^+ = \frac{w^+}{E} \left[\frac{cm^2}{V \sec}\right]$$

It is specific to each ion type moving in a given gas. For example $\mu^+ = 1.72$ for CO_2^+ moving inside Argon gas and $\mu^+ = 1.09$ for CO_2^+ moving inside CO_2 Gas [20].

The mobility of electrons, except for very low fields, is not constant. In fact, due to their small mass, electrons can substantially increase their energy between collisions with the gas molecules under the influence of an electric drift field E_{drift}. In a simple formulation, one can write the drift velocity, as:

$$w_e = \frac{eE_{drift}}{2m}\tau \left[\frac{cm}{\mu \sec}\right]$$

Where τ is the mean time between collisions and m the electron mass.
At high fields, a typical value of w_e is around 5cm/μsec, which is roughly 3 orders of magnitude faster than the ions' w^+ under similar conditions [20].

Since the charge motion involves collisions with the gas molecules, their drift under an electric field should involve diffusion. While the ion diffusion is negligible due to their mass, electron's diffusion is an important parameter, which influences the accuracy of the localization and time measurements in gaseous detectors. The transverse diffusion (perpendicular to E_{drift}) strongly influences the detector resolution and the longitudinal one affects the time resolution of the signal. As a function of the drift distance from the origin *d*, the diffusion width of the electron cloud $\tilde{\sigma}$ increases according to:

$$\tilde{\sigma} = \sqrt{\frac{2\varepsilon_k}{e(E/p)}}\sqrt{\frac{d}{p}}.[cm^2]$$

With ε_k being the characteristic energy of the electron in the gas and is a function of the reduced electric field *E/p*.

The diffusion along and across the drift direction is varying among the gases, and typically for a 1cm drift under 0.5kV/cm in atmospheric pressure it ranges between 0.1mm RMS in CO_2 to 2mm RMS in Argon [20].

2.3 excitation and ionization of gas molecules

At electric fields above a few kV/cm, electrons gain enough energy between successive collisions, to cause excitations and ionizations of the gas molecules. The excitations result, among others, in photon emission; these photons can create secondary electron emission, perturbing the process of detection (photon feedback). Adding complex molecules to noble gases, such as hydrocarbons which have radiation-less transitions, will absorb these photons and therefore will reduce secondary effects. Photon emission in some noble gases, known as efficient "gas scintillators", is employed for radiation detection [21]

When the energy of an electron increases over the first ionization potential of the gas E_i the result of the impact can be gas ionization, namely the creation of a new electron-ion pair; the primary ionization electron continues its transport in the gas. The probability of ionization is rapidly increasing above the ionization threshold, on the account of gas excitations; it reaches a maximum, for most gases, around electron energy of 100 eV.

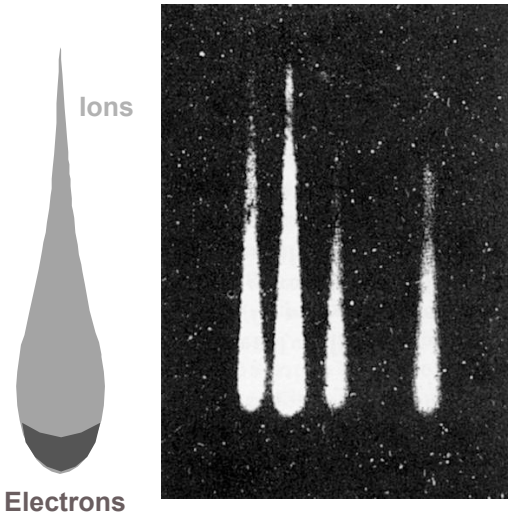

Figure 4: Photograph of an electron avalanche in gases [20]. The positive ions are left behind the fast electron front.

The process of ionizations by electron collisions is the basis for the avalanche multiplication. After a mean free path ℓ electron-ion pair will be produced, and the two electrons will continue to generate, again after one mean free path, two additional electron-ion pairs and so on. If n is number of electrons at a given position and n_0 is the number of electrons at X=0, after a path X, the increase in the number will be exponential:

$$M = \frac{n}{n_0} = e^{\frac{X}{\ell}}$$

Where, M represents the multiplication factor.

The Townsend coefficient $\alpha = \ell^{-1}$ is a function of the electric field E and as seen in Figure 5 the detected charge depends on the potential difference V_0 that is applied on the electron inside the gas medium. At very electric fields (E<1kV/cm), charges begin to be collected, but recombination is still the dominant process. In the ionization chamber region, at higher electric fields (kV/cm), full collection begins. At electric fields above few kV/cm, multiplication starts and the detection charge is proportional, through the multiplication factor M, to the original deposited charge. At higher electric fields, this proportionality is gradually lost, as a consequence of the electric field distortions due to the large space charge created. This region reaches saturation gain, where the same signal is detected independently of the original ionizing event. At even higher electric fields it is the Geiger-Muller region, where the photon emission process begins to propagate avalanches in the counter, and the full length of the detector becomes a sheath of electrons and ions.

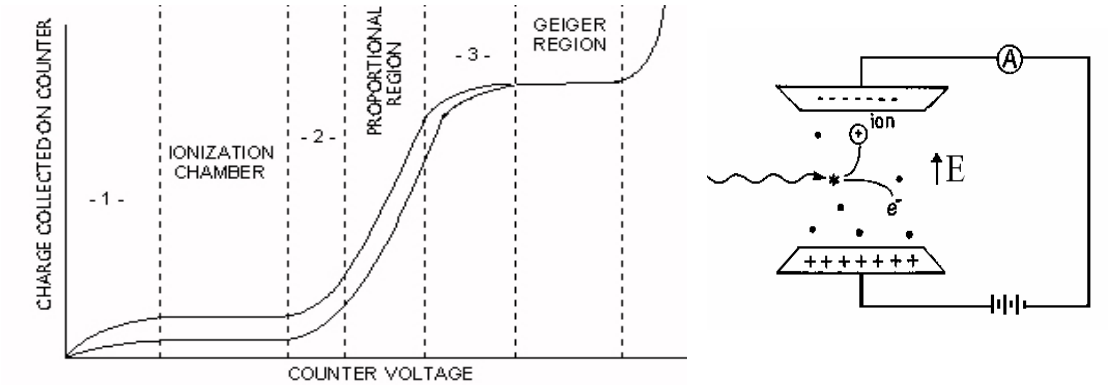

Figure 5: Left: Gain-voltage characteristic for parallel-plates counter, showing the different regions of operation. Right: schematic view of the parallel-plates configuration.

Secondary processes, like photon emission inducing the generation of avalanches spread over the gas volume, photon- and ion-induced secondary avalanches and space charge deformations of the electric field (which is strongly increased near the front of the avalanche), eventually result in spark breakdown. It is interesting to note that such radiation-induced sparks, which limit the operation of modern detectors, were used for optical recording of particle-tracks in the early days of particle physics experiments. A phenomenological limit for multiplication before breakdown is given by the Raether condition [20]:

$$M \sim 10^8$$

The statistical distribution of the energy of electrons, and therefore of M, in general does not allow one to operate at average gains much above 10^6 if one wants to avoid breakdowns. However, a multiplication process inside holes, as discussed in details at the next section, reduces dramatically these secondary effects and therefore allows reaching higher gains. Using the THGEM, stable operation was indeed obtained at gains above 10^7.

2.4 Multiplications inside holes

Electron multiplication inside holes is attractive because the avalanche confinement in the hole strongly reduces secondary affects, particularly that due to ion- and photon-induced secondary electrons. Hole-multipliers can therefore reach higher gains, compared to "standard" wire chambers, parallel-plate, resistive-plate, microstrip and other "open-geometry" detectors. [22,23] Cascaded hole-multipliers permit total blocking of photon-feedback effects, which permit operating them even in noble gases that emit very high photon yields. Avalanche ions, flowing in a direction opposite to that of the electrons in gaseous detectors, induce gain-limiting and field-distorting secondary effects. Recent cascaded hole-multipliers developed at our group in cooperation with the Coimbra university permit reducing the flow of back flowing avalanche ions by 3 orders of magnitude [46].

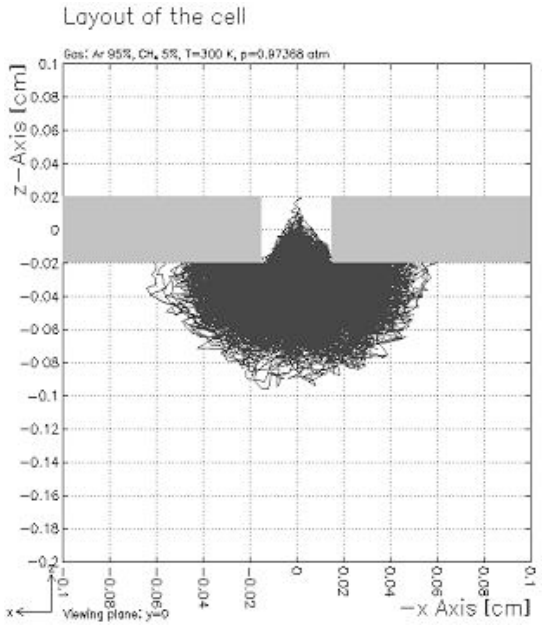

Figure 6. Garfield [31] simulation of a single electron multiplication (Gain~10^3), inside the |THGEM hole.

The hole-multiplier provides true pixilation in radiation localization. Each hole acts as individual multiplier, which is separated from other avalanches. Garfield [31] simulation of a single electron multiplication (Gain~10^3), inside the |THGEM hole is shown in figure 6. As will be shown, the multiplication reaches values as high as 10^5 in a single THGEM multiplier; cascading several multipliers results in stable operation at gains above 10^7.

2.5 A short survey of hole based detectors

Hole based multiplication has been a subject of numerous studies in a large variety of applications. In 1973 Breskin and Charpak introduced a glass track chamber, constructed of an array of tiny (~1mm diameter) glass capillaries filled with neon/helium gas [4]. It is a simple detector based on recording optically light emitted following the electrical gas discharges created in the capillaries, upon the gas ionization induced by charged particles. The particle tracks were formed by a succession of discharges confined within individual 50mm long glass capillaries of about 1mm in diameter.

At 1980 Lum et al. investigated the detection of gamma rays, using "lead-glass" converters, made by fusing glass tubes stacked to form a close packet array [5]. The glass tubes had 1.4mm ID, 1.6mm OD and were 2mm thick, filled with Ar/CH_4 (70:30) at 1 Atmosphere. The gamma rays interacted with the glass converter, which yielded conversion electrons escaping into and ionizing the tube-gas. The ionizing electrons drifted along the tube gas, in an electric field; they were detected in a multiwire proportional chamber (MWPC) placed below the tubes. In order to provide a uniform drift field, the glass was treated in an elaborate hydrogen reduction process that provided a high-resistivity (~500MΩ) surface layer. A photon conversion efficiency of 8% was achieved with 511 keV Gamma rays.

Del Guerra et al introduced high resistivity lead-glass tube arrays for RICH counters [6]. The glass tubes were coupled to a MWPC; an electric field of a few kV/cm

applied along the tubes permitted some multiplication within their volume. The glass tubes (0.91mm ID, 1.1mm OD and 1cm thick) reached a gain of 10 and 100 for 4.7kV in Ne+He+4%C_2H_6 (760 Torr) and 4.2kV in Isobutene (40 Torr) respectively. They were found to be efficient preamplification elements and as a UV shield, cutting more than 99% of the UV light. However, the electron transmission through the arrays has not been optimized (~60%).

Sakurai et al. introduced a new type of proportional counter, using capillary plates [8]. It consisted of a bundle of fine glass capillaries with electrodes in both sides. The capillaries were 100 microns in diameter and 800 microns in length. Gas gain of 10^4 was measured in Argon/CH_4 (95:5) at voltages of 1480V and 1080V at 760 and 380 Torr respectively. Using 5.9 keV x-rays and with a gas gain of 7000, an energy resolution of 25% FWHM was obtained.

In 1996 Sauli introduced the gas electron multiplier (GEM) [10]; as mentioned above it comprises 50-70 microns diameter holes etched in a 50-micron thick metalized Kapton foil. It operates in a large verity of gases including noble gas mixtures, providing a gain of 10^4 in a single element and gain exceeding 10^6 in cascade of 3-4 elements. The avalanche process is fast (ns) and generally free of photon mediated secondary effects. The GEM is the most attractive and extensively studied hole multiplier. An intensive research of the GEM has been carried out in our group at the Weizmann Institute. It was focused towards the understanding of the properties of **cascaded GEM multipliers** [24] and their use as **photon detectors** for the UV and visible spectral range [25, 16, and 11], **x-ray imaging** [26] and **neutron detection** [27]. Derived from the GEM is the Micro-Hole & Strip Plate (MHSP) multiplier, which after a multiplication in GEM-like holes further multiplies the avalanche electrons on thin anode strips deposited on its "bottom" electrode [28]. Cascaded GEM and MHSP multipliers provide high gains and permit the efficient blocking of avalanche ions [29, 46].

As part of the study of hole-multipliers, another multiplier was investigated by Peskov et al., called the "optimized GEM" [9, 13], made of mechanically drilled holes in a G-10 plate metalized on its both sides. It reached gains of 100 and 10^4 for particles and x-ray respectively inside Argon/Isobutane (95:5), and inside pure Xe; with the use of a CsI photocathode the maximum gain achieved was 10^3.

Our THGEM [1,2,3] introduced in 2004 is the most recent development in gaseous hole-multipliers. It is a simple and robust device for atmospheric and low-pressure applications, where moderate sub-mm localization is sufficient.
It has fast response and reaches very high gains of 10^5 and 10^7 in single- and double-THGEM configurations at atmospheric pressure and 10^4 at very low pressures, e.g. at 1 Torr of isobutane. It has a rate capability of 10^7 events/mm^{2}sec at a gain of 10^4 and an energy resolution of 20% FWHM for 6 keV x-rays, which is similar to that of the standard GEM. We will discuss in the following the methodology of our studies and provide the results in detail.

3. Methodology

The present study encompasses the production of THGEM electrodes, calculation of electric fields by MAXWELL software package [30], the simulation of electron transport by GARFIELD software [31] and the measurement of various operation properties of the THGEM.

3.1. THGEM production procedure

The THGEM electrodes (Figure.2) were produced in the Printed Circuit Board (PCB) industry [32], by standard drilling and etching process, out of G-10 plates. We used double-sided copper-clad plates, of thickness t = 0.4 – 3.2 mm; the insulator was first drilled with a hexagonal pattern of holes of diameter d (d ~ 0.3 – 2 mm) and pitch a (a ~ 0.7 – 4 mm) and then the copper was etched at a 0.1mm distance around the hole's rim (Fig.2). A large assortment of THGEM electrodes was produced by this very economic method; table 1 summarizes the various THGEM geometries studied in the present work.

Table 1. A summary of the geometrical parameters of THGEMs studied in this work.

THGEM#	Thickness t [mm]	Drilled hole diameter d [mm]	Etched Cu diameter d+2h [mm]	Pitch a [mm]	Ref PC area [%]
1	1.6	1	1	7	98
2	1.6	1	1	4	94
3	1.6	1	1.2	4	92
4	1.6	1	1.2	1.5	42
5	3.2	1	1.2	1.5	42
6	2.2	1	1.2	1.5	42
7	0.4	0.5	0.7	1	56
8	0.8	0.5	0.7	1	56
9	0.4	0.3	0.5	0.7	54
10	0.4	0.3	0.5	1.0	77
Standard GEM	0.05	0.055	0.07	0.14	77

3.2. MAXWELL and GARFIELD simulations

Maxwell is 3D software, which solves Maxwell equations for a given geometry and voltage configuration. It was used to calculate the electric fields (direction and values) above, below and inside the THGEM holes and to evaluate the field at the THGEM surfaces; the latter is important for the operation of THGEM-based photon detectors with *reflective* photocathodes deposited on their top surface. This helped us to understand the role of each field and thus to optimize both the THGEM dimensional parameters and the operation conditions.

Designing the THGEM configuration with Maxwell is done in four stages:

1. Drawing the geometry, which is actually a unit cell of the THGEM, composed of two quarters holes as shown in figure 7. Duplication of this unit-cell results in the full geometry of the THGEM.
2. Assigning materials, such as conductors to the electrodes and insulators to the substrate. The THGEM upper and lower surfaces are assigned as perfect conductors and used as electrodes. The THGEM's insulator is assigned as FR4 glass epoxy, which is equivalent to the G-10.
3. Applying voltage sources to the electrodes, such that it simulates the experiments. The THGEM bottom is usually chosen to be grounded, and other voltages are applied according to the experimental conditions.
4. Creating the calculation mesh, which determines how precise should the calculation be at any given point. The mesh can vary from region to region. Usually around 25,000 mesh points are divided as follows: holes - 10,000; G-10 - 3,000; electrodes – 4,000; background – 8,000. This division can change according to the significance of the simulation e.g. for examining the electric field on the THGEM top surface, more points will be added at this electrode.

After the mesh is defined, the software solves Maxwell equations, and the results are given at a post process stage as 2D and 3D plots, as shown below in section 4.1.

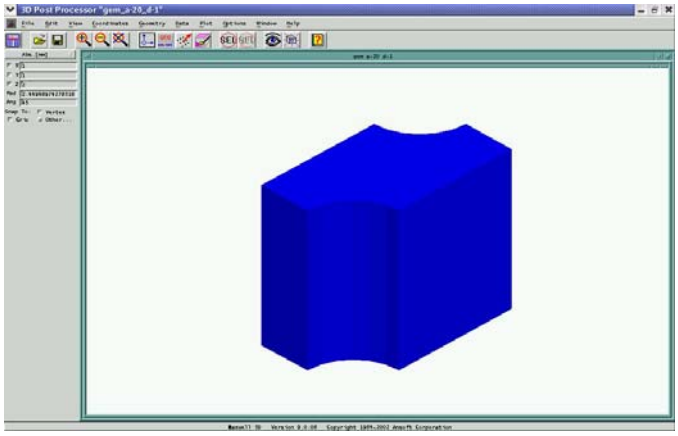

Figure 7: Maxwell simulation of the THGEM unit cell geometry. Duplication of this unit-cell results in the full geometry of the THGEM.

The electric-field maps, calculated by Maxwell, are transferred into the Garfield simulation package. In addition to Maxwell's map of fields, Garfield takes into account also the gas type and pressure. According to the cross sections of the gas, the drift of the charges has a certain probability for collisions and ionizations. While Maxwell calculates the electric fields, Garfield simulates the full electron and ion paths including diffusion, and the electron multiplication inside the holes, as seen in figures 8 and 14.

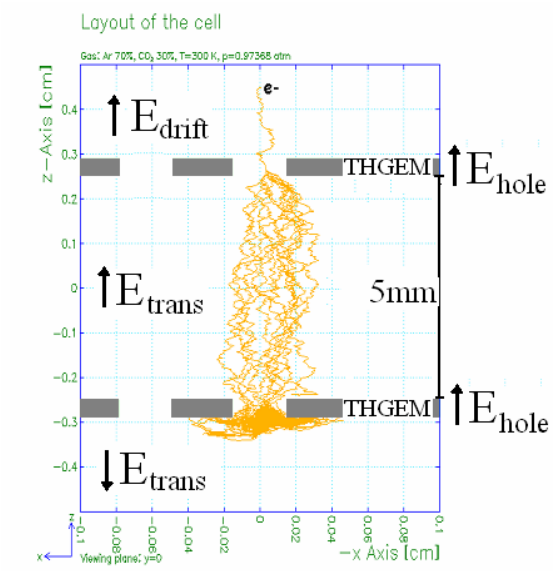

Fig.8 – GARFIELD simulation of the avalanche process in a double- THGEM #9 detector, in atmospheric pressure Ar/CO_2(70:30); with ΔV_{THGEM}=1350 V, the multiplication factor of each THGEM is ~30, resulting in a total gain of ~900.

3.3. Experimental techniques

All measurements, except the x-ray energy resolution, were carried out with photoelectrons emitted from a CsI PC, irradiated with UV light from a continuous Ar(Hg) lamp or from a spontaneously discharging H_2 lamp. The experimental setups for the different measurements are described below. The PC was either a thin (30nm) ST film, vacuum deposited on a Quartz window, pre-coated with a very thin (20-30nm) under-layer of Cr, or a thick (300nm) Ref film, vacuum deposited on the THGEM's top face. The ST mode with the PC placed 10 mm above the multiplier, represents indeed the operation mode of a THGEM coupled to any source of electrons located in the gap above it; besides the photomultiplier configuration, it could be a conversion gas gap for ionizing particles in a tracking detector or in a TPC, an x-ray conversion gap or another multiplier preceding the THGEM.

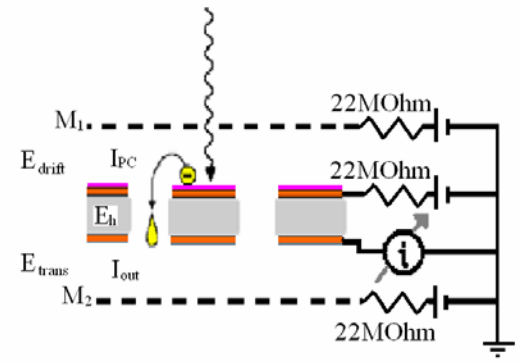

Figure 9: Scheme of the DC current measurements using reflective photocathode. The power supply is connected in series to a 22MOhm resistor that protects the THGEM in case of sparks.

We used an individual power supply for each electrode, as shown in figure 9, permitting to independently vary the different fields. A current limit of 50nA was usually set on the power supplies biasing the THGEMs (CAEN, model N471A); a 22MOhm serial resistor was added to limit eventual discharge currents. The light-source intensity was tuned with a series of absorbers placed in front of the lamp, adopting the light flux to the THGEM gain, within the above-mentioned current limits. Except for the electron transfer efficiency (ETE) and x-ray energy resolution, all measurements were carried out by recording the current from various electrodes in the different experimental setups. The current was measured on electrodes grounded through the precision electrometer (KIETHLY 610C), permitting recording currents down to 10 pA; the currents on powered electrodes were measured indirectly by recording the voltage drop across a known resistor, which permitted measuring currents in the range of 10nA to 100 nA. The precision of these measurements was of 1% and 5%, respectively.
At very low THGEM voltages, below the multiplication threshold, the ETE can also be derived from the currents measurements, by comparing I_{OUT}, the output current of the THGEM (i.e. collected on the interconnected THGEM bottom and mesh M2 electrodes – figure 8) to I_{PC}, the photocurrent emitted from the PC (measured at the PC with a field E_{drift} established and no multiplication in the THGEM). But, as soon as the multiplication in the holes starts, this current measurement is no more valid for the ETE assessment; we cannot separate the ETE from the effects and charges resulting from the multiplication process [33]. In this range, the ETE was measured in a pulse-counting mode that permits separating the two processes. It is based on recording single electron pulses, in which case electron transfer inefficiency is directly translated to counting rate deficiency. We used a relative measurement, comparing the counting rate in the examined system to that recorded in a reference system known to have 100% ETE. This is done, of course, under exactly the same experimental conditions, with identical PC, UV-light illumination, and total pulse-gain and electronics chain. The pulse-counting method was used to obtain the transfer efficiency of the THGEM with either semitransparent or reflective PCs, in various gases. The details are given in [24,33] and in section 3.3.2 below.

3.3.1 Effective gain measurement

Effective gain, the product of the absolute multiplication factor in the holes and the Electron Transfer Efficiency was measured in different gases, in various THGEM geometries(table 1), at atmospheric and low pressure; it was assessed both in a single- and double-element cascaded modes.

The measurements were done in DC current mode, using continues Ar(Hg) UV lamp, as explained above. Each electrode is connected to a CEAN (model N471A) power supply, using a maximum limit of 50nA, and a strong resistor of 22MOhm in line, to protect the THGEM in case of sparks.

The measurement procedure is composed of two stages, as shown in Fig.10:

1. Measurements of the Normalization current (the current leaving the photocathode).
2. Measurements of the total current reaching the THGEM bottom electrodes

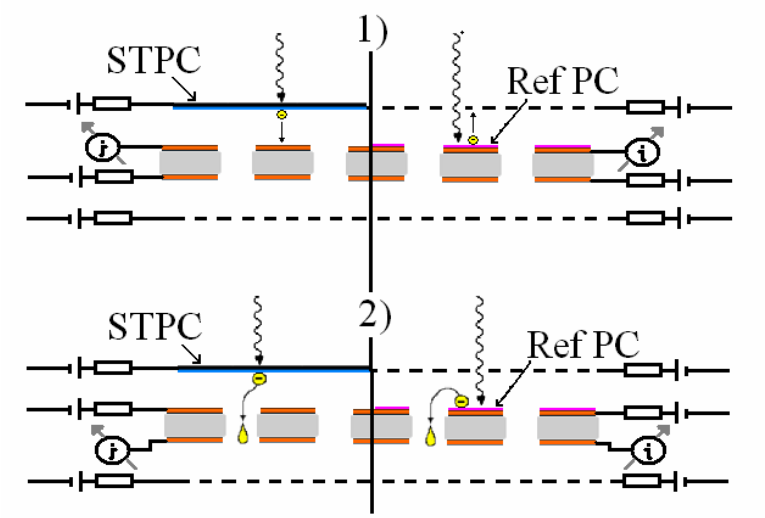

Figure 10: Schematic view of the effective gain measurement setup. 1) Normalization current setup 2) Multiplication current setup. Left: using semitransparent photocathode. Right: using reflective photocathode placed on the THGEM top surface.

Dividing the total current by the normalization current gives the average multiplication factor of a single electron. This method can not separate between the ETE and the real gain; e.g. for 10 electrons leaving the PC, the current measurements will show the same result when all of them enter the holes and multiply by factor 10, and when only 5 of them enter the holes and multiply by 20. Therefore it is called an *effective gain*.

In cases where the gain is not sufficient it is possible to cascade two THGEMs, by mounting them at a distance of a few mm, and applying a strong transfer field (~3kV/cm) between them, to ensure the extraction of electrons from one THGEM to the next. The normalization measurement is the same as in single-THGEM mode, and the total multiplication current is measured on the second THGEM bottom. Double-THGEM operation results in higher gain and better stability, since each THGEM operates at lower voltage, farther from its spark limit.

3.3.2 Electron Transfer Efficiency (ETE)

The Electron Transfer efficiency is the probability to focus the electron from its creation point into a hole. This is an important parameter for any hole-multiplication detector, affecting its operation; e.g. the detection efficiency of single-electron events or the energy resolution of charged particles or x-rays inducing ionization electrons in the conversion gap preceding the THGEM. The ETE depends on the detector's operation mode and conditions; it was measured in various gases as function of the THGEM operation voltage in single-multiplier geometry.

We have measured the ETE and its dependence on the THGEM voltage, in two basic configurations:

a) *Ref PC,* in which the single electrons originate from a PC deposited on the top surface of the multiplier and the field E_{drift} above it is set to 0. In these E_{drift} conditions, like in a reflective-GEM [33,34], the photon detector has a considerably

reduced sensitivity to ionizing particle background. In this configuration we also measured the ETE dependence on E_{drift}.

b) *ST* PC, in which the single electrons originate from a PC placed a few mm above the THGEM electrode, with a field E_{drift} between them; in this configuration the measured ETE is relevant for *ST* photon detectors (with E_{drift} >0.5 kV/cm) and for tracking detectors and TPCs (with E_{drift} typically in the range of 0.1kV/cm). It is also relevant for the understanding of the operation mechanism of two THGEMs in cascade, where avalanche electrons created in the first multiplier should be efficiently focused into the second one.

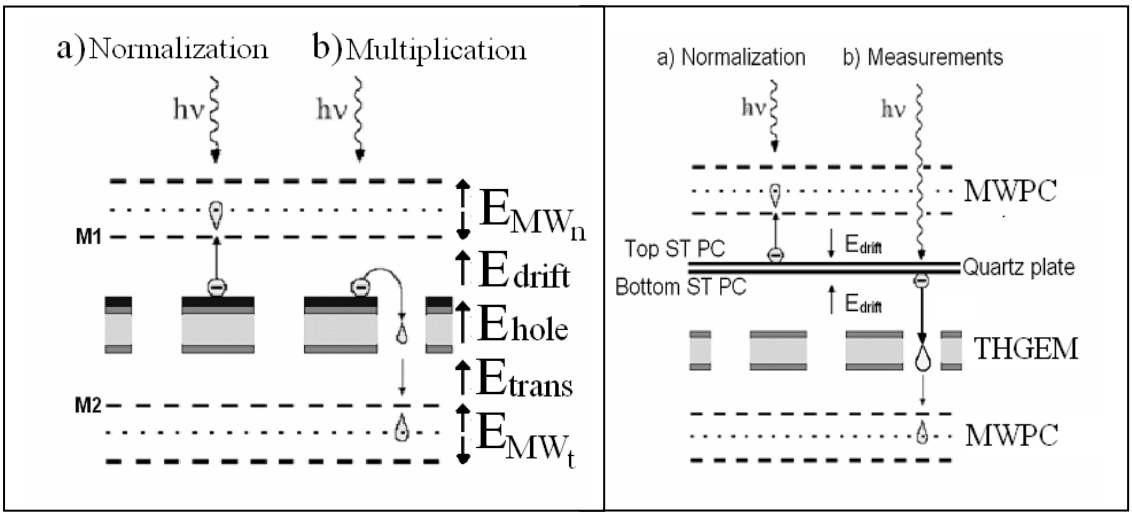

Figure 11: The experimental setup for the Electron Transfer Efficiency measurements in a reflective (left) and semitransparent (right) photocathode modes. The multiplication pulses were measured on the lower MWt and the normalization pulses on the upper MWn.

Fig. 11 (left) depicts the ETE measurement setup and method for *ref* PC, which has two steps: first we set E_{drift} = -3kV/cm and measure the event rate originating from electrons created at the *Ref* PC and multiplied at the top MWPC anode, (MW_{nor} - normalization). The high E_{drift} ensures full photoelectron extraction efficiency; the electric field established on the MW side of the mesh M1 is higher than 6kV/cm, ensuring full electron transfer through M1. We may thus assume that in this configuration the ETE is 1. Then, with the same light flux and electronics chain, we set E_{drift}= 0 and measure the event rate originating from electrons entering the THGEM and being multiplied in a cascade: first in the holes and further in the bottom MWPC anode (MW_{trans} - transfer). (This arrangement permits varying the THGEM gain while keeping a fixed total gain on the cascade). The ratio of event rates (n_{trans}/n_{nor}) provided us with the ETE.

Figure 11 (right) depicts the experimental setup and method for measuring ETE with *a ST* PC. Similarly to the *Ref* PC mode described above, we had a normalization and a measurement step, and we used the ratio of event rates in both steps to provide the ETE. However, the normalization included a further step, as we had two 20nm thick

CsI layers deposited on both faces of a thin quartz plate, pre-coated with 2.5nm thick Cr. First we measured the ratio of photocurrents recorded simultaneously under the same UV illumination and the same extraction field E_{drift}, from both sides of the quartz plate; this provided us with the photocurrents ratio R_I between the top *Ref* PC and the bottom *ST* PC. Then we preceded as above and measured the rate of events recorded in the defined pulse-height window, for events originating from the top *Ref* PC and amplified in the top MW_{nor}. Finally the event rate was measured within the same pulse-height window and under the same illumination, for events originating from the *ST* PC and multiplied in the THGEM and the MW_{trans} in cascade, maintaining the same total detector gain and electronics chain. The ratio of the two event-rates, normalized by the photocurrents ratio R_I, provided us with the ETE, as function of ΔV_{THGEM} and of E_{drift}

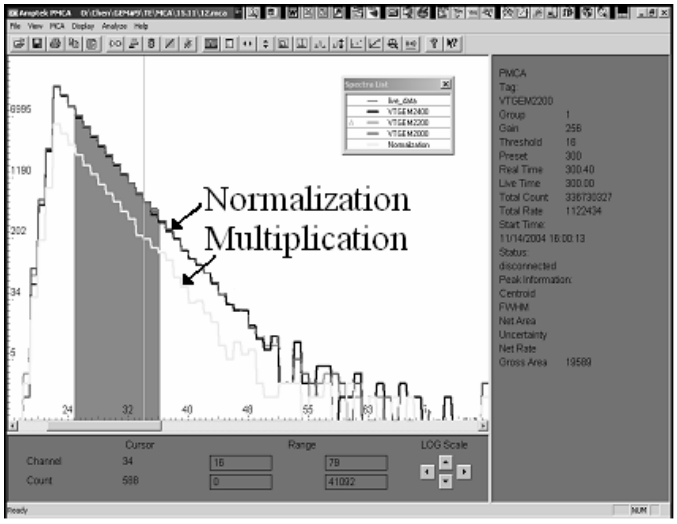

Fig. 12: The single-photoelectron spectra with the window for integrating. The identical slopes of the THGEM multiplication and the normalization measurements indicate that they have the same gain. The shown THGEM multiplication curve has less counts for an equal counting time, which results for ETE<1 in these conditions.

The validity of the measurement relies on the assumption that in both cases the single-electron pulse height is exponential, following the Polya relation without saturation

$$p(q) \cong (q / Mq)e^{-(q/M)}$$

With, M being the total gain and *q* the number of electrons in the avalanche.

Therefore it is important to adjust the total gain in both measurement steps to be identical within 2-5%, by comparing the slopes of the exponential distributions. Furthermore, we measured the event rate within a given window (Figure 12), set in the middle of the pulse-height distribution, safely above the noise and below the tail, to avoid counting secondary or pile-up pulses. The method is no more valid in cases where the multiplication process is strongly affected by secondary or quenching processes and the distribution fails to follow the exponential relation. For a more detailed discussion of this method refer to [24].

3.3.3 Counting-rate capability

The pulse-height dependence on the event rate is important for high-rate applications, and due to the reduced number of holes per mm^2 compared to standard GEM, each hole contains higher electron flux, and this could be of a concern. The measurements were done in two steps, as seen in figure 13, with a *Ref* PC deposited on THGEM1, and a mesh placed a few mm above it.

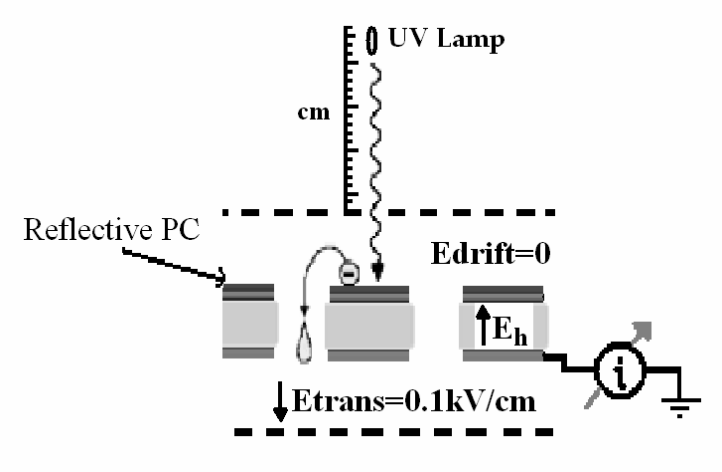

Figure 13: The experimental setup for the counting-rate response measurements in a reflective photocathode mode. The current was measured on the THGEM bottom, and the UV rate was determined by the distance between the lamp and the photocathode.

A collimated UV lamp illuminated a PC area of 7 mm^2. First, the photocurrent I_0 was measured as a function of the UV intensity on M1 with both sides of THGEM1 interconnected and with E_{drift}=3kV/cm. This provided the photoelectron rate per unit area. Then E_{drift} was set to 0, THGEM1 was biased with ΔV_{THGEM} to a known gain and the current I_1 was recorded at THGEM1 bottom, with a reversed E_{trans}, again as function of the UV intensity. I_1/I_0 provided the gain of THGEM1 and its dependence on the impinging photoelectron flux. The same measurement was performed with two THGEMs in cascade, operating in symmetric mode (same operation voltages) and having Etrans= 3kV/cm. The current I_1 was now measured at the lower THGEM bottom, with a reversed field underneath.

3.3.4 Ion Back Flow (IBF)

As the avalanche develops inside the THGEM holes, the ions drift towards the photocathode or towards the electrons creation point; the process is called ion back flow. It is one of the potential damaging factors that can cause aging to the photocathode. Ions hitting the photocathode can also cause the emission of secondary electrons, which lead to secondary avalanches.

The ion back flow fraction (IBF) is measured relative to the electron multiplication current reaching the THGEM bottom. It is assumed that under the operational condition, most of the electrons are being collected at the THGEM bottom, and therefore the IBF can be estimated as the fraction of the total ion avalanche that is drifting back to the photocathode.

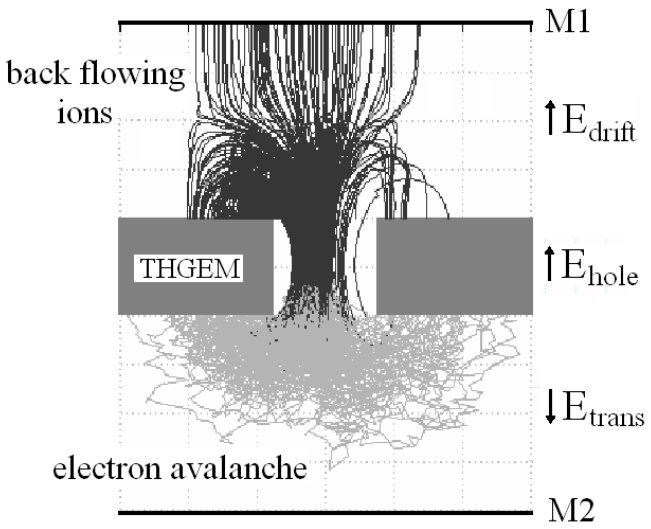

Figure 14: The experimental setup for the ion back flow measurements in a semitransparent mode, and the simulated path of the electron and ions. The current was measured simultaneously on the THGEM bottom, on the THGEM top and on the upper mesh M1.

The IBF was measured (figure 14) on the upper mesh and on the THGEM top relative to the total multiplication current that reaches the THGEM bottom. It was measured as a function of E_h and as a function of $E_{drift.}$ The measurement is similar to the effective gain measurement and being conducted under the same conditions i.e. DC current mode measured with a Pico-Ampere Meter. The ratio between the current at the photocathode and the current measured at the THGEM bottom is the IBF.

3.3.5 X-ray energy resolution

The energy resolution measured with an x-ray source irradiating a small THGEM surface (7mm^2), as in fig 15, is determined mainly by the gain homogeneity over the surface of the electrode and, to less extent, by the ETE homogeneity over that surface.

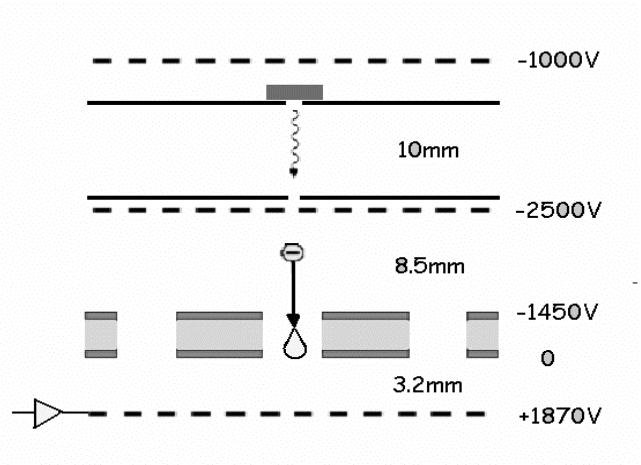

Fig. 15: X-ray measuring scheme; the collimator focuses the beam on a small area of 7mm2; the x-rays are absorbed in the 8.5mm gap. The electrons are focused into the holes, are multiplied and collected on an electrode below.

A 5.9 keV ^{55}Fe X-ray source, attached to a collimator of 3mm hole diameter and 10mm length, was installed inside the Ar/CH4 (95:5) filled gas vessel, facing the THGEM and placed 8.5 mm above it. These x-ray photons have an absorption length of 10mm in the gas; each photon releases about 200 electrons. Pulses from the bottom of the THGEM were recorded, via a charge-sensitive preamplifier (ORTEC 142) and a linear amplifier (ORTEC 570), on a multi-channel analyzer.

4. Results and discussion

4.1. Maxwell & Garfield simulations

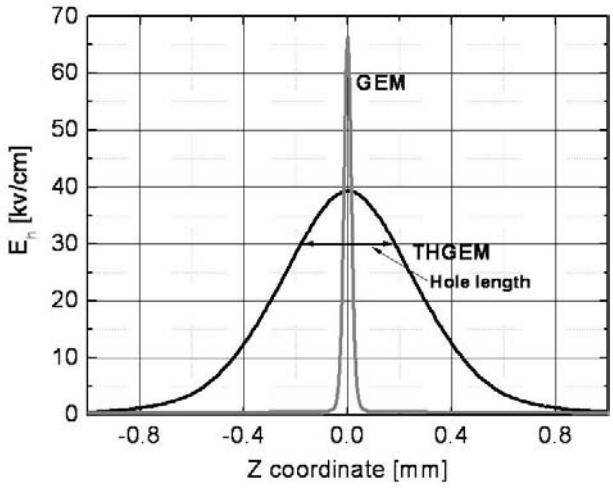

Figure 16: MAXWELL software calculation results of the electric field strength along the central axis of a standard GEM and a THGEM hole, for maximal operation voltages in Ar/CO2 (70:30). THGEM#9: ΔV_{THGEM}=2kV; Standard GEM: ΔV_{GEM}=0.5kV.

MAXWELL and GARFIELD simulations were found to be very useful for understanding the general role of the various geometrical parameters of the THGEM electrode and for comprehending their operation mechanism and the expected performance.

MAXWELL calculation results of the electric field strength E_h along the hole's central axis, for THGEM#9 (Table 1), with ΔV_{THGEM}=2kV, are shown in fig.16. It reaches a maximum of ~40 kV/cm at the middle of the hole and remains above the multiplication threshold (10-15 kV/cm) along an additional ~ 0.3 mm distance outside the hole; it indicates that the gas multiplication will typically slightly extend out of the hole under the maximal 2 kV bias. Other calculations showed that the avalanche will be fully confined within the hole at ΔV_{THGEM} =1.3kV. A similar effect was noticed with a standard GEM in noble gases [35], showing evidence for the avalanche extending-out by much more than the hole radius.

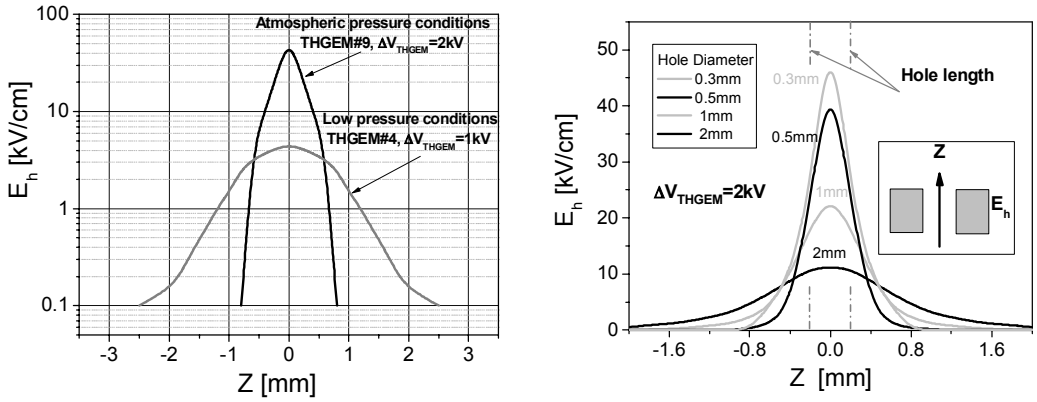

Figure 17: MAXWELL calculation results of the electric field strength along the central axis of the THGEM hole. Left: optimal conditions for atmospheric and low pressure (10 Torr). E_h at atmospheric pressure is factor 10 stronger comparing to low pressure conditions. Right: for a fixed plate thickness t=0.4 mm and different hole diameters. With decreasing hole diameter the field increases and is more confined within the hole. Experimental measurements show maximum gain for t/d ~ 1, as shown below in the gain measurement results.

Figure 17 Shows the results of MAXWELL calculation of E_h in atmospheric pressure conditions comparing with low pressure conditions (left) and for a THGEM with t=0.4 mm, for different hole diameters (right). With decreasing hole diameter, E_h increases and becomes more confined within the hole. The resulting performance in terms of maximal E_h (and therefore the expected gain) shows an optimum for t/d= ~ 1, as will be discussed in the paragraph describing the low pressure gain results.

MAXWELL/GARFIELD calculations gave us another insight into the operation mechanism, as for example to the effect of the transfer field. In Fig. 8 the avalanche is simulated in a cascaded double-THGEM#9 in Ar/CO_2(70:30), with ΔV_{THGEM}=1350V on each multiplier and a high (3 kV/cm) transfer field between them. At ΔV_{THGEM}=1350V the multiplication is~30 (this low gain was chosen for the sake of clarity of the figure); the total calculated gain is~900. This is a surprisingly high total gain equal to the product of the two individual gains. With higher ΔV_{THGEM} and E_{trans} values the calculated total double-THGEM gain exceeds the product of the two individual ones.

MAXWELL/GARFIELD provided the clue for this effect, showing that the high transfer field modifies the field near the hole's end (fig. 18), thus modifying the multiplication factor. The effect is expected to be significant at the higher ΔV_{THGEM} values, where the avalanche further extends out of the hole. Furthermore, from GARFIELD calculations it is clear that a high transfer field is responsible for the efficient extraction of electrons from the first THGEM towards the second one in a cascade; the large hole size together with the extension of the field out of the hole is responsible for an efficient focusing of the electrons into the second THGEM. As will be shown in the next section this was confirmed experimentally.

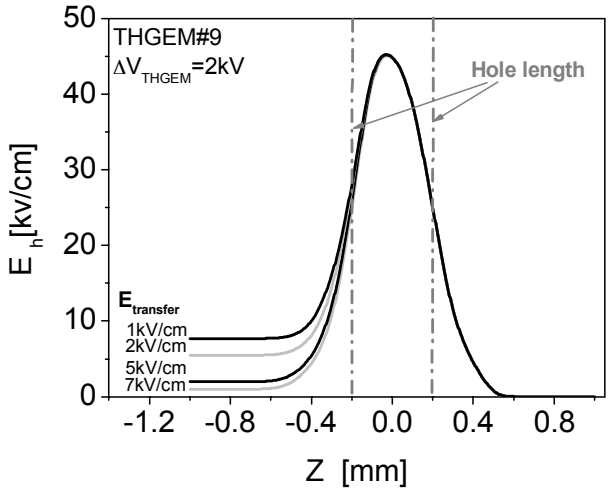

Figure 18: MAXWELL calculation results of the electric field strength E_h along the hole axis in the presence of an external field E_{trans}. A high E_{trans} applied above or below the THGEM may significantly affect E_h and the multiplication factor, outside the hole.

The electric field on the top surface of the THGEM is shown in fig 19, along the line interconnecting two adjacent hole centers, for various ΔV_{THGEM} values. For ΔV_{THGEM} >800 V the field exceeds 3 kV/cm all over the surface. Under this relatively high electric field, in a multiplier layout with a *ref* PC, the photoelectron backscattering in the gas is low [36] this guarantees its efficient extraction from the *Ref* PC into the gas.

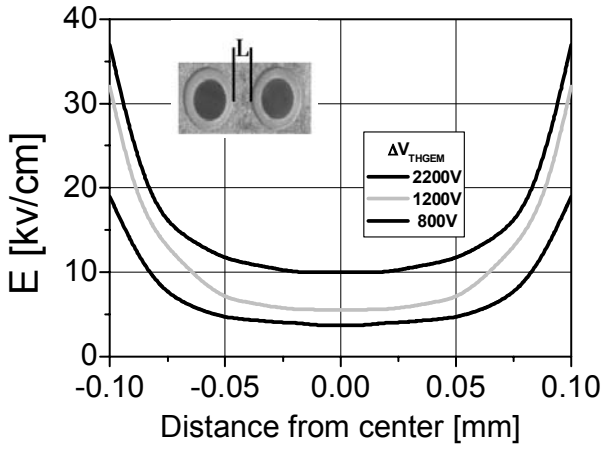

Figure 19: Maxwell calculations of the electric field on THGEM#9 top surface, E_s, along the axis interconnecting two hole centers. The electric field magnitude is above 3kV/cm, even at ΔV_{THGEM} = 800V.

4.2 Effective gain

The experimental method for assessing the THGEM gain was explained above; the experimental schemes are given above for both detector configurations with *Ref* and *ST* PCs, and for double-THGEMs. The gain results for low pressure and atmospheric pressure are shown in figures 20-27 and in figures 29-31 respectively, for various THGEM parameters.

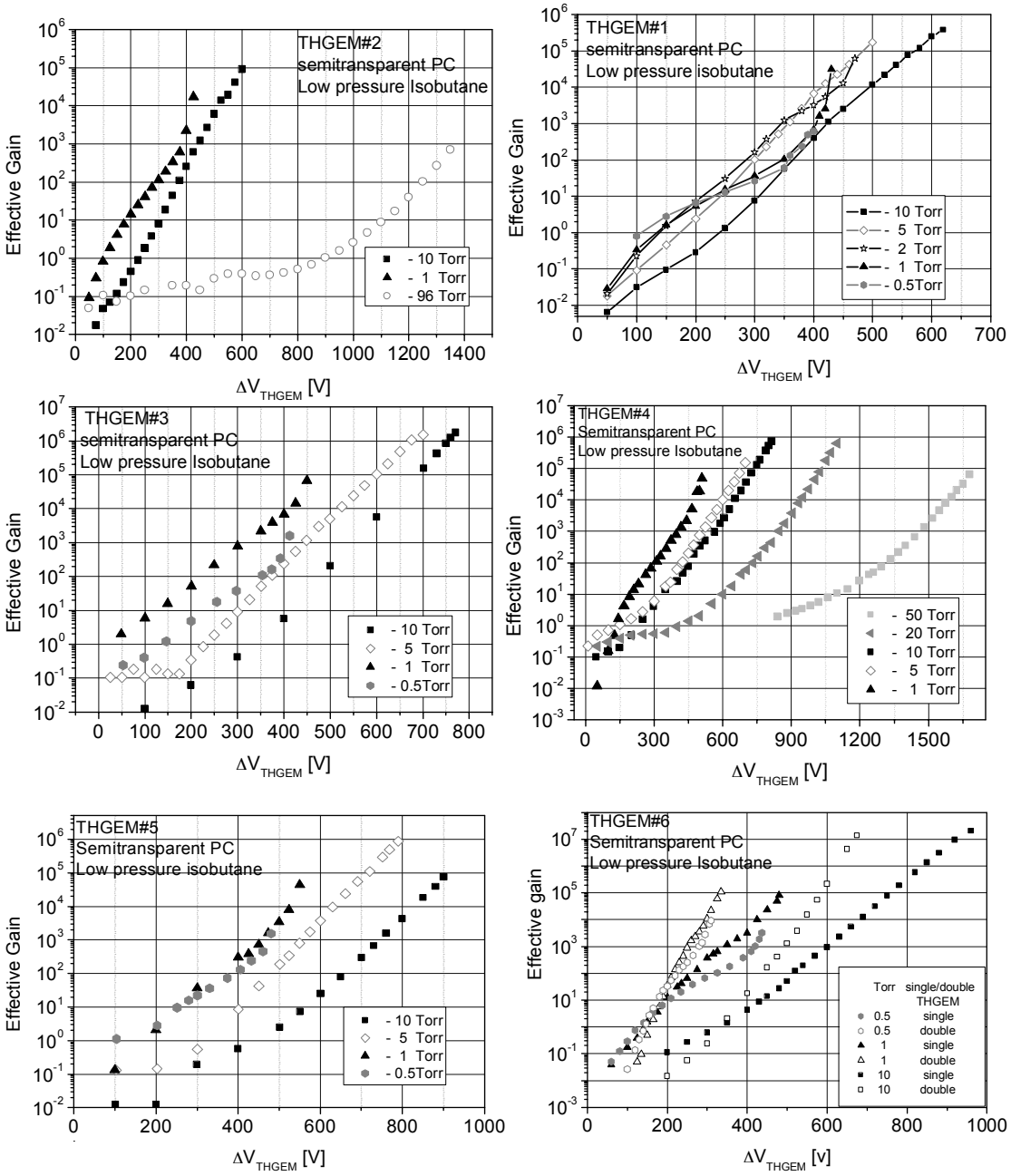

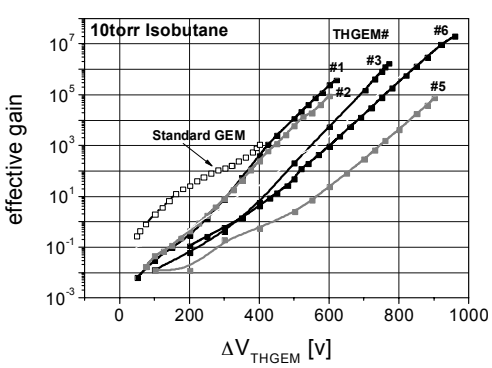

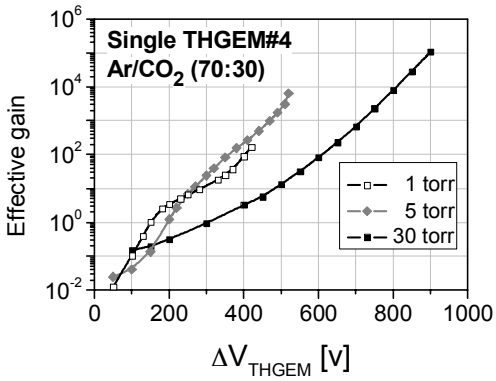

Figures 20-27: Absolute effective gain results at low pressure Isobutane and Ar/CO_2 (70:30) at different THGEM geometries according to table 1. The highest gains were measured on THGEM#6.

Figures 20-27 summaries the results of the effective gain measurements inside low pressures gas. Six different THGEM geometries were investigated in isobuthane and Ar/CO_2 (70:30), at low pressures of 0.5,1,5,10 and 100 Torr. The higher gain results obtained with THGEM#6, which reached gains of 10^5 and 10^7 at 1 and 10 Torr respectively.

These effective gain results are higher by a few orders of magnitude compared to measurements we have done using a standard GEM at low pressure, as shown above. When cascading double THGEMs, inside low pressure gas, we found it necessary to maintain a distance of at least 10mm between the THGEMs, for allowing efficient focusing of the electrons inside the second THGEM's holes.

.

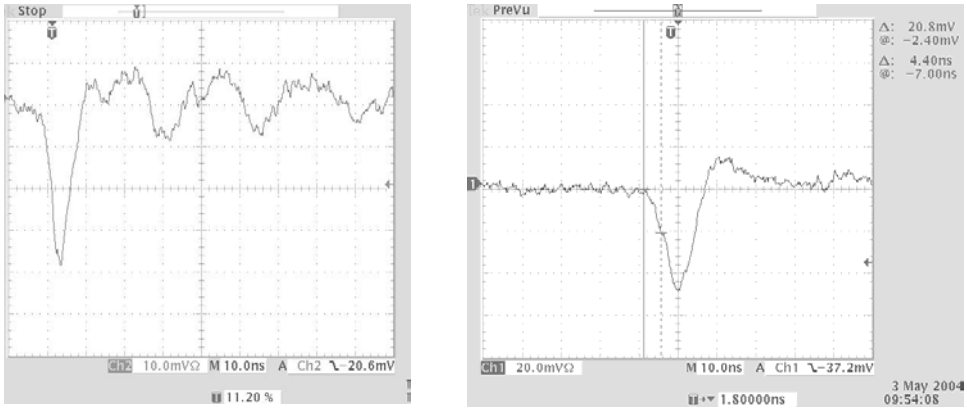

*Figure 28: A fast single-photon pulse. Left: 5ns rise-time, measured in double-THGEM#4 in 1 Torr isobutane at gain ~6*10^5. Right: 8ns rise-time, measured in double-THGEM#7 in 740 Torr Ar/CH4 (95:5) at gain >10^6.*

The high gain obtained with the THGEM, permitted recording single-photoelectron signals with a fast current amplifier (Fig 28). The relatively fast multiplication process yields pulses with a rise time of ~5ns and ~8ns at low pressure and atmospheric pressure respectively. It is probably due to the faster drift velocity of the electrons and ion in the higher reduced electric fields (E/p) in these conditions. The THGEM was found to be very stable and very robust for the low-pressure operation; not even a single THGEM was damaged during our extensive measurements.

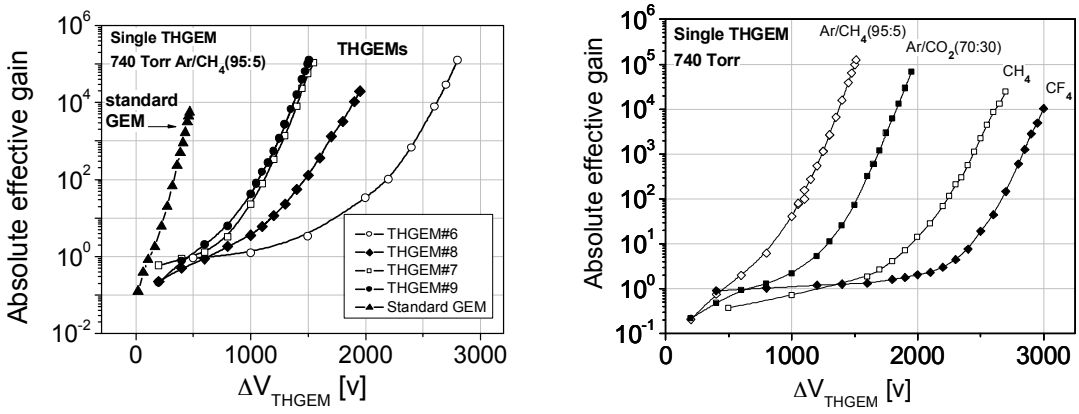

Figures 29: Absolute effective gain results at 760 Torr. Left: comparing between THGEM geometries and the standard GEM shows much higher gains at the THGEMs. Right: results of THGEM#9 at different gases in 740 Torr.

Fig. 29 (left) demonstrates that a single THGEM provides up to a 10-fold higher effective gain than a standard GEM. The maximum gain is naturally reached at different ΔV_{THGEM} values, according to the multiplier's geometry. Fig. 29 (right) shows the absolute effective gain of THGEM#9 in various gases; the highest effective-gain values, ~10^5, were reached in standard mixtures employed in GEMs; CF_4, which is an important gas for applications in windowless Cherenkov detectors [34,36], yields a maximum gain of 10^4, though at very high ΔV_{THGEM} values. Fig. 30 shows the gain of a double-THGEM#9 in Ar/CH_4 (5%) at E_{trans} =3kV/cm and in Ar/CO_2(30%), at E_{trans} values of 1 and 3kV/cm; at 3kV/cm, the double-element multiplier yields up to 100-fold higher gains compared to that of a single-multiplier, reaching total effective gains of ~ 10^7. Other electrodes were tested, e.g. THGEM#10, providing similar results. As will be discussed below in section 3.3, at the effective-gain values above a few hundreds, the ETE reaches 100% and therefore the effective gain is equal to the true gain within the holes.

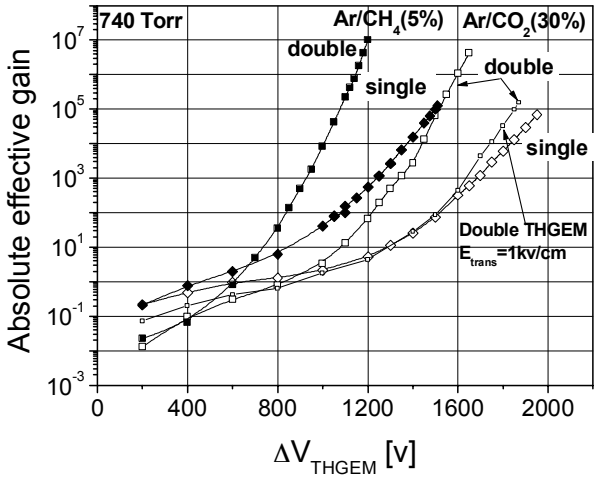

Figure 30: Absolute effective gains of single- and double-THGEM#9 multipliers, in Ar/CH_4 (5%) at E_{trans} =3kV/cm and in Ar/CO_2(30%), at E_{trans} of 1 and 3kV/cm;

The effect of E_{trans} on the total gain is demonstrated in figure 30, showing that double-THGEM gains exceeding the product of two individual gains are obtained with a high E_{trans} and high ΔV_{THGEM} values. This was tested in various gases and with different electrode configurations, showing systematically a similar behavior [3]. The double-THGEM structure provides very high total gains, while the voltages on each element are far from the sparking limit, which permits a more stable operation. It was noted that the most stable double-THGEM operation is the symmetric one, namely with both elements biased at equal operation voltages. We also noted that the 0.1 mm etched Cu around the drilled holes is essential for achieving high gain. An attempt to operate a THGEM electrode, in which such etching was not done, resulted in ~10 times smaller gain.

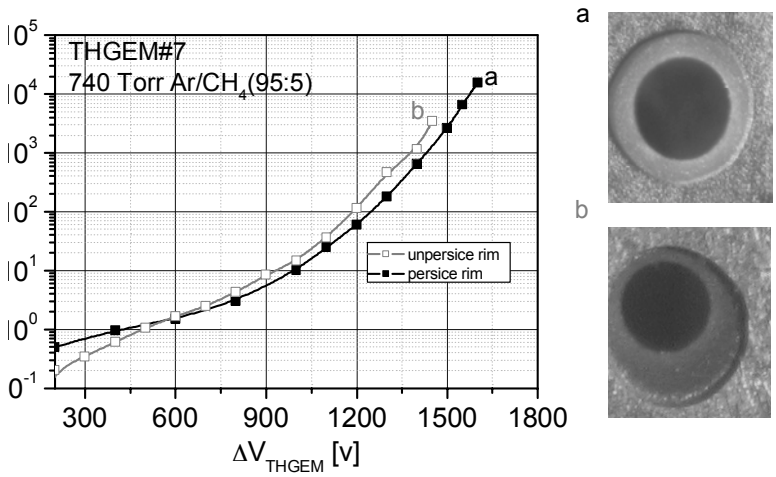

Figure 31. Absolute Effective Gain measurements, using a THGEM with a) centered (upper photo) and b) unscented Cupper holes, which demonstrate the importance of the 0.1mm rim between the G-10 and the Cupper holes.

It is also important to have the etched and drilled patterns precisely centered. In our case the precision was ~ 20μm . Electrodes in which the etched pattern was displaced from the drilled one by more than that did not function properly, and yielded up to10-fold smaller maximal gain, as seen in figure 31.

The pitch of the THGEM was found to have a minimal effect on the gain. For example, the onset of the multiplication in THGEM#10, having a pitch of a=1mm, started a few tens of volts lower than in THGEM#9, with a pitch a=0.7mm. Both multipliers reached similar maximum gains in Ar/CO_2 (70:30) [3-I]. The effect was systematically observed also at the low-pressure range [3-II]. There is no clear explanation at the moment and it does not seem to be supported by any MAXWELL calculation.

4.3. Electron Transfer Efficiency

The results of the ETE with *Ref* PC on a THGEM#9 in four gases investigated in this work are shown in fig.32 as function of ΔV_{THGEM}. Full transfer efficiency is obtained at rather low gains, of 3-30, according to the gas filling. This could be compared to a standard *reflective* GEM, in which full ETE was attained only at high gains, above 500 in Ar/CH_4 (95:5) and above 5000 in pure CF_4 [33]. The reason is the denser hole area (holes occupying 46% of the area, compared to 22% in a GEM) and the larger hole diameter (here 300 microns compared to 50-70 microns in a GEM). Due to the larger hole size, which is indeed larger than the electron diffusion (~100μm for 1 cm [20]) electron focusing into the holes is more efficient and is typically obtained at smaller gains compared to that of a standard GEM.

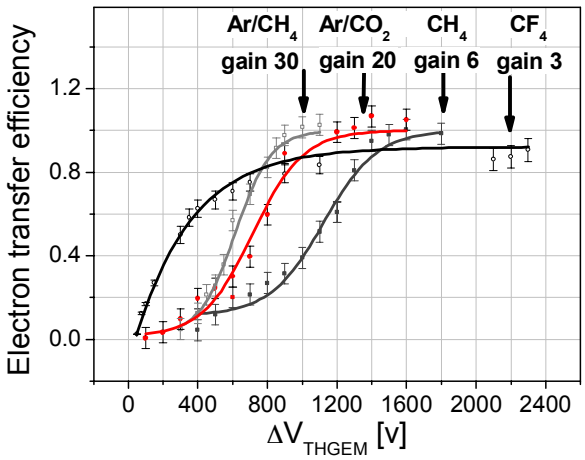

Figure 32: ETE measured with THGEM#9, as function of ΔV_{THGEM} in a reflective photocathode mode, in various gases; full transfer efficiency was achieved at significantly lower gain compared to the standard GEM [33].

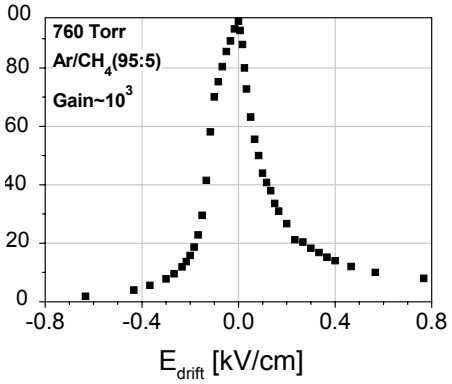

Figure 33: ETE measured with THGEM#9, as function of E_{drift} in Ar/CH_4 (5%); maximum ETE was obtained at E_{drift}=0.

In fig. 33 we show the dependence on E_{drift} of ETE of THGEM#9 with *ref PC* in Ar/CH_4 (95:5). Like in a GEM [33] full transfer efficiency was measured for E_{drift}=0. Setting E_{drift} at slightly reversed (negative) value will reduce the detector's sensitivity to ionizing background, as all ionizing electrons will drift away from the multiplier. This was recently demonstrated with a hardon beam [34].

The ETE results in the *ST* PC mode for THGEM#9 are shown in figure 34 (left) as function of ΔV_{THGEM}, for two gases. These data were obtained by the current recording method in the voltage range below the multiplication onset, and by the pulse-counting method in the multiplication range. Full transfer efficiency was attained in Ar/CO_2(30%) and in pure CH_4 already at small respective gains of 10 and 20, with E_{drift}= 0.3 V/cm. As in standard GEM the electron focusing into the holes, and thus the ETE, is expected to drop when the ratio E_{drift}/E_{hole} increases. The ability to maintain full ETE at higher E_{drift} was measured for THGEM gains of 10, 10^3 and 10^4, as seen in figure 34 (right). A drop is observed at E_{drift} values above ~3kV/cm and ~5kV/cm for gains of 10 and 10^3-10^4, respectively.

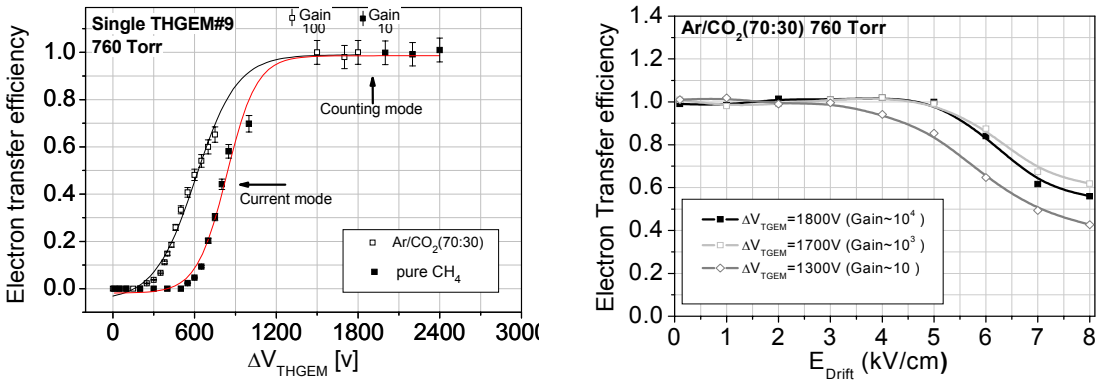

Figure 34: ETE of THGEM#9 in the semitransparent photocathode mode. Left: Inside Ar/CO_2 (70:30) and in pure CH_4. Full ETE is reached at respective gains of 10^2 and 10. Right: ETE as function of E_{drift}; Ar/CO_2 (70:30) at different gains.

As discussed above, the ETE measured with a *ST* PC is relevant also for the operation of a cascaded-THGEM structure. The results of fig. 34 (right) confirm that even with transfer fields between two cascaded elements as high as 3kV/cm, a full electron focusing into the second THGEM holes can be obtained.

In analogy to standard GEM operation in cascade, the charge transferred to the second element depends not only on the ETE discussed above but also on the electron extraction efficiency from the first multiplier into the gap between them. This efficiency is expected to increase with E_{trans}/E_{hole}. Its dependence on E_{trans} was measured in a double THGEM configuration similar to that shown in fig. 7, with a ST PC. First we measured the current I_B collected at the bottom of THGEM1, with a reversed E_{trans}, and then we measured the current I_T on the top of THGEM2, with its top and bottom interconnected, as function of E_{trans}. The ratio I_T/I_B, provides the electron extraction efficiency. Experimental data are shown in figure 35 for Ar/CO_2 (70:30). At a gain of 10^4 full extraction efficiency from THGEM1 is achieved at E_{trans} >4kV/cm in this gas.

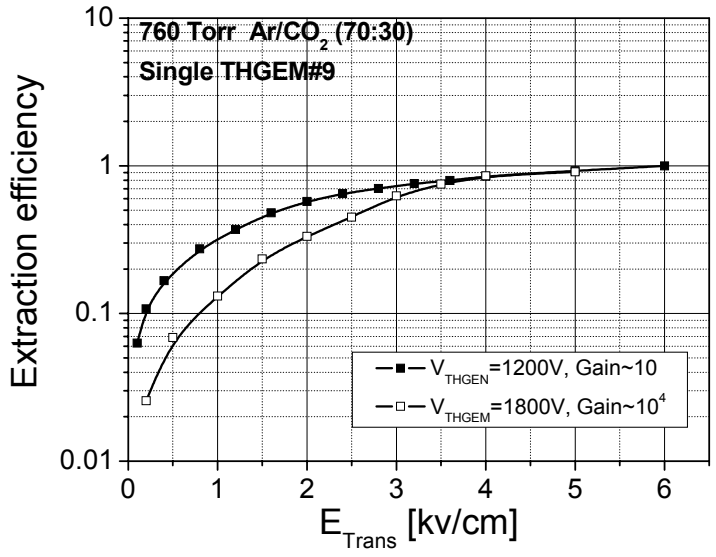

Figure 35: Electron extraction efficiency from THGEM#9 at gains of 10 and 10^4 in Ar/CO_2(70:30), as function of E_{trans}.

4.4 Counting rate capability

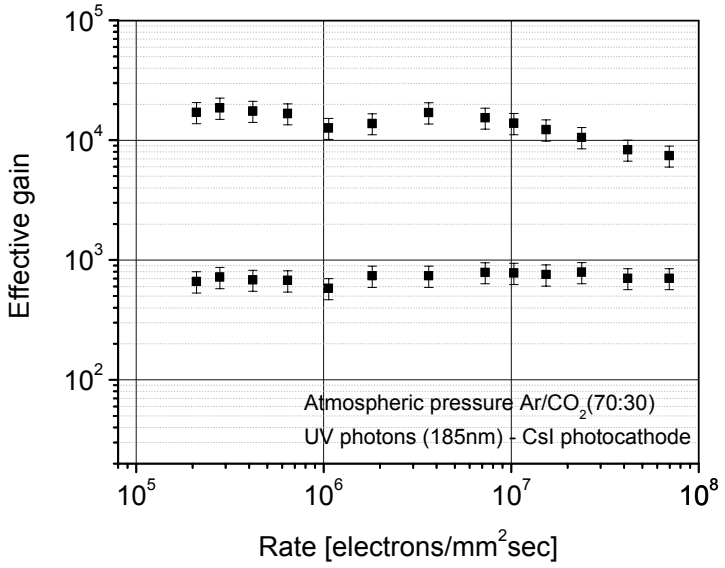

Figure 36: Counting rate response to single photoelectrons, of THGEM#9 with reflective photocathode, in single- and double-THGEM configurations.

The results of the gain stability with the counting rate, measured with single UV photons, are shown in Fig. 36. They show a flat response within the following photoelectron flux measured: up to $8x10^7$ electrons/mm^2 sec with a single THGEM#9 at an effective gain of ~10^3 and up to 10^7 electrons/mm^2 sec with double THGEM#9 at a gain of 10^4.

The maximum measured event rates in these experiments were limited by our source intensity, therefore the results only represent a lower limit.

The results could be compared to that of a standard GEM operated at a gain of 10^4, irradiated with 5.9keV x-rays, where the pulse-height was constant up to a total event rate of 10^5 converted x-rays/mm^2 sec [37]. Assuming about 250 electrons per x-ray this corresponds to ~ $2.5*10^7$ electrons//mm^2 sec. Thus the lower limit of rate capability achieved with the THGEM, is similar to that measured in the standard GEM.

4.5. Ion Backflow (IBF)

IBF, the fraction of total avalanche-induced ions that are collected at the cathode, is relevant both for TPCs and for gaseous photomultipliers incorporating a solid PC. In the first case the ions are causing dynamic field distortions. In the second case the ions create PC physical and chemical aging; they also induce secondary electron emission from the PC, resulting in secondary feedback pulses that limit the detector performance. A discussion on the ion backflow in gaseous detectors, its consequences and methods for its reduction is given in [46]. In the present work we have measured IBF for single- and double-THGEM structures, with *Ref* and *ST* PCs; the latter is the one relevant for TPCs.

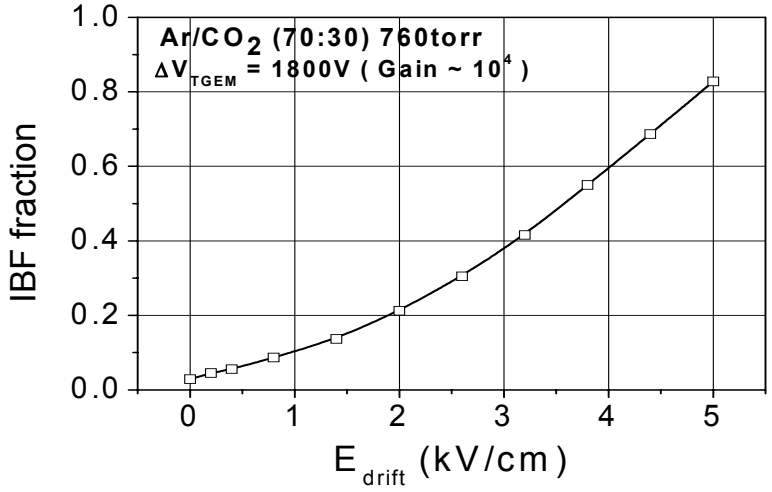

Figure 37: The Ion backflow fraction to a semitransparent photocathode, of a single THGEM#9, as function of E_{drift}.

The IBF for a single THGEM#9 measured with a *ST* PC is shown in figure 37 as function of the field E_{drift} above the THGEM. The fraction of avalanche-induced ions which drift towards the photocathode is less than 2% at E_{drift}=0 and increases almost linearly with E_{drift}. These data imply that in double-THGEM operation with E_{trans}~3kV/cm between both THGEMs, less than 40% of the ions will be flowing from the second THGEM towards the first one. Out of this, part may be trapped at the first THGEM bottom electrode, thus reducing the IBF as compared to that in a single THGEM operation. The IBF graph shown in Fig. 37 was measured at a gain of 10^4.

4.6 X-ray energy resolution

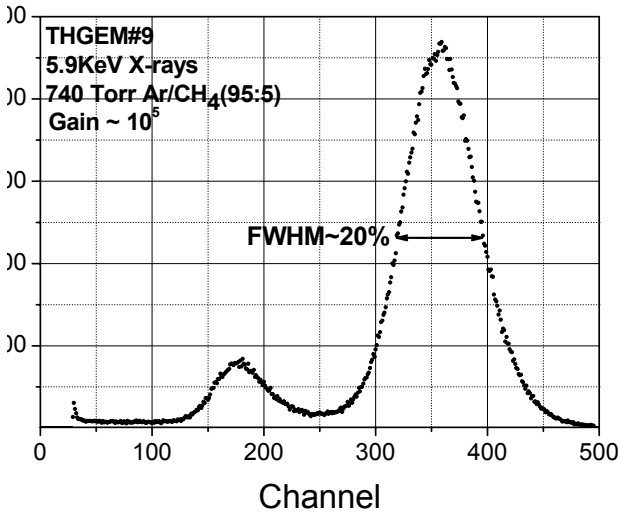

Figure 38: An energy spectrum recorded with 5.9 keV ^{55}Fe X-rays in a single-THGEM#9; 740 Torr Ar/CH_4 (95:5), gain 10^5.

The energy resolution for 5.9 keV ^{55}Fe x-rays was measured with THGEM#9 in 740 Torr Ar/CH_4 (95:5), with a collimated source irradiating an area of ~7 mm^2. A conversion gas gap of 8.5 mm was added in front of the multiplier, with a drift field of 1.25kV/cm. The detector was operated at a gain of 10^5. Pulses from the bottom electrode of the THGEM were recorded, via a charge-sensitive preamplifier (ORTEC 142) and a linear amplifier (ORTEC 570), on a multi-channel analyzer (fig 38); the resolution is ~20% FWHM. For comparison, a resolution of 18% FWHM was recorded with 5.9 keV x-rays in a standard GEM at a gain of 1000 in Ar/DME(80:20) [37]

5. Summary

The THGEM developed in this M.Sc. thesis work is an attractive robust and economic electron multiplier, suited for applications at **atmospheric gas pressure** requiring large area detectors with single-electron sensitivity and moderate (sub-mm) localization resolution. The high attainable gains, of 10^4 –10^5 in a single multiplier and 10-100 times higher in a double-THGEM multiplier, are due to the reduced photon- and ion-feedback processes. The THGEM has stable operation in a variety of gases including pure CH_4 and CF_4. The rapid avalanche process developing across the hole results in fast signals, of few ns rise-time; the counting-rate capability is exceeding MHz/mm^2 at a gain of 10^4. THGEM's can be coupled to both gaseous ionization volumes and to solid radiation converters; in the latter configuration the converter can be placed above the THGEM or deposited directly on its top face. In both cases the radiation-induced emitted electrons are efficiently focused into the multiplication holes. X-rays were detected with a gas converter with an energy resolution of ~20% FWHM at 5.9 keV. The solid converter material can be chosen according to the application; it can be a photocathode in gaseous photomultipliers [33], an x-ray converter (e.g. CsI) in secondary-emission x-ray imaging detectors [39] or a neutron converter (e.g. Li, B, Gd, polyethylene etc.) in thermal-or fast-neutron imaging detectors [40]. Such detectors for fast-neutron imaging are under development at our group.

From our systematic study we may conclude that the operation mechanism as well as the role of the various electric fields involved in the THGEM operation is rather similar to that known for standard GEMs.

In particular, we observed the following similarities and differences:

- The maximal voltage difference across the THGEM does not scale with the dimensions and the field inside the holes is smaller than in a GEM; but due to the larger dimensions, particularly the larger thickness, significantly higher gains are obtained. Furthermore, due to the larger hole-size (larger than the electron diffusion) electron focusing into the holes is more efficient and is typically obtained at smaller gains compared to that of a standard GEM.

- In our study of the role of each field we have confirmed that with a *Ref* PC the field E_{drift} above the THGEM should be 0, to have maximum focusing into the holes; it can be kept slightly reversed to reduce the sensitivity of detectors with solid converters to ionizing background.

- Unlike a GEM coupled to a *ST* PC, in which E_{drift} should be kept moderate to avoid diverting the drifting electrons towards the metallic GEM surface, the large holes in the THGEM permit an operation with very high E_{drift} values; an efficient photoelectron focusing into the holes even at drift fields of 5kV/cm was measured with THGEM#9 at a gain of 10^4. This is important for the efficient extraction of photoelectrons or radiation-induced secondary electrons, particularly in noble-gas mixtures, where backscattering into the converter is high at low fields [41].

- The dipole field within the holes deflects the avalanche electrons towards the bottom face of the THGEM, but with a strong E_{trans} underneath the THGEM electrode the charge is efficiently diverted and transferred into the following multiplier in the cascade. In standard cascaded GEMs this is an important issue of optimization, since

with an E_{trans} too high the electrons will not be focused into the second GEM, while an E_{trans} too low will not extract the electrons from the first one [24,33]. With the large holes in the THGEMs, electron focusing into the second THGEM remains effective even with very high E_{trans} values, as with the high E_{drift} values discussed above.

- As a result, a double-THGEM operation was proved very efficient and stable in all tested gases, providing high total gains. Very high E_{trans} values, of several kV/cm, could be applied to increase the transfer efficiency and thus the total gain. In some cases, at high THGEM voltages and with a high E_{trans} value between the two elements, the total effective gain exceeded the product of the two individual ones. This peculiar feature is occurring firstly because the extraction of charges from the holes into the next stage is very efficient and reaches almost 100%; furthermore, because the dipole hole-field is extending out by about the hole's diameter, at large gains part of the avalanche is developed outside the hole, thus being susceptible to modifications by any strong field in the gaps around the THGEM. The extension of the avalanche outside the hole might have undesirable consequences, such as coupling of neighboring avalanches between the two elements and instability due to photon-mediated processes. Thus care should be taken to choose the appropriate operation conditions, such as THGEM geometry and applied voltages, specific for each application, in order to avoid these phenomena.

- Just as in a standard GEM, the flow of back-drifting ions is strongly related to that of the avalanche electrons. THGEMs seem to have more efficient electron transport, and not surprisingly also more efficient ion transport, as compared to GEMs. This could be a point of concern for applications where ion backflow is highly undesirable. Reducing ion backflow in THGEM cascades is the main subject of our ongoing research, attempting to apply the idea of reversed-bias multi-hole & strip electrodes (R-MHSP), recently shown [46,42] to reduce the ion backflow fraction IBF by a factor of ~10^3 when incorporated in a cascaded structure.

At low pressure Isobutane very high gains of 10^5 and 10^7 were reached at 1 and 10 Torr respectively, and a gain of 10^4 in 5 Torr Ar/CO_2 (70:30). An important range of applications exists at low gas pressures, down to the sub-Torr values, for which the THGEM might be a very appropriate solution. Examples are in detection of heavily ionizing radiation with very low penetration, e.g. heavy particles in nuclear physics; another example is in the detection of low-energy ions, recently proposed by us [43] for tracking nanodosimetry applications. Ions are deposited by the incident radiation in a small low-density gas bubble that simulates a relevant biological target; the detected ions should provide information on the number of ionizations and their spatial correlation, deposited in this gaseous DNA-like model-target [44]. For this purpose an ion detector has to be developed that operates at low-density gas, in the sub-Torr range; the THGEM electron multiplier might be an important part of this ion detector. The successful operation of the THGEM at sub-Torr values has an important potential for this application.

In summary, the THGEM can be easily produced, spanning a large scale of geometrical parameters: we have tested such electrodes with thickness ranging from 0.4mm up to 3.2mm, and with hole sizes and distances in the same range. By varying the thickness and the hole size it is possible to optimize the THGEM for various operation conditions, as for example the operation at very low gas pressures, in the

mbar range [1, 2]. Similarly, varying the holes pitch affects the ETE and thus permits optimization of the electrode to a particular operation layout. The holes pitch also affects the localization precision provided by this electrode, and some optimization with regards to the localization demands are also possible here. The localization properties of 100x100 mm^2 THGEM detectors are the subject of another work [45].

Though the gain in single-and double-THGEMs is high, further improvements could be achieved by using different geometries. One example is using smaller hole diameter, where according to calculations, E_h can reach much higher values. Conical holes shape, like in the standard GEM, may also be tested. In applications for charged-particle detection, where the fraction of the cupper area is less important, a larger rim between the cupper clad and the hole's edge might result in higher stability. As shown in figure 30 the rim is a crucial parameter for reaching high multiplication.

For UV-photon imaging in RICH applications, where the detector operates in CF_4, the G-10 substrate failed reaching high gains following discharges. This was attributed to possible damages caused by Fluor radicals to the glass fibers of the G-10 material. An attempt to use copper claded Kevlar, instead of G-10 did not provide satisfying results so far. Other materials, less sensitive to CF_4, should be tested.

References

[1] R. Chechik et al.: Thick GEM-like hole multipliers: properties and possible applications Nucl., Instr. and Meth. A535 (2004) 303-308

[2] R. Chechik et al.: Thick GEM-like multipliers - a simple solution for large area UV-RICH detectors., http://arxiv.org/abs/physics/0502131

[3] C. Shalem et al.: Advances in Thick GEM-like gaseous electron multiplier – part I: atmospheric pressure (to be submitted to Nucl., Instr. and Meth) part II: low pressure (to be submitted to Nucl., Instr. and Meth)

[4] A. Breskin et al. : A glass track chamber, Nucl. Instr. and Meth. IO8 (1973) 427-429

[5] G.K. Lum et al.: Lead oxide glass tubing converters for gamma detection in MWPC., IEEE NS27(1980)157.

[6] A. Del Guerra et al.: High resistance galss tubing for RICH counters and for electromagnatic calorimeters., Nucl. Instr. and Meth. A257(1987)609

[7] R. Belazzini et al.: The Well detector., Nucl. Instr. and Meth. A423(1999)125

[8] H. Sakuray et al.: A new type pf propotional counter using a capillary plate., Nucl. Instr. and Meth. A374(1996)341

[9] V. Peskov et al.: First attempts to combine capillary tubes with photocathodes., Nucl. Instr. and Meth. A433(1999)492

[10] F. Sauli :GEM: A new consept for electron amplification in gas detectros., Nucl. Instr. and Meth. A386 (1997) 531-534

[11] A. Breskin et al.: Recent advances in gaseous imaging photomultipliers. Nucl. Instr. and Meth. A513(2003) 250.

[12] T. Meinschad et al.: Detection of primary and field-enhanced scintillation in xenon with a CsI-coated GEM detector., submitted to Nucl. Instr. and Meth. A513(2003) 250.

[13] L. Periale et al.: Detection of the primary scintillation light from dense Ar, Kr and Xe with novel photosensitive gaseous detectors., Nucl. Instr. and Meth. A478(1999)377.

[14] J. Va'vra.: Novel photon detectors for RICH applications., Nucl. Instr. and Meth. A502(2003)172.

[15] S. Roth : Charge transfer of GEM structures in high magentic fields., Nucl. Instr. And Meth. A535(2004)330.

[16] A. Breskin et al.: Advances in gas avalanche photomultipliers. Nucl. Instr. and Meth. A442 (2000)58.

[17] A. Di Mauro, et al.: photoelectron backscattering effects in photoemission from CsI into gas media. Nucl. Inst. And meth A371(1996)137

[18] A. Breskin, CsI UV photocathodes: history and mystery. Nucl. Instrum. And Meth. A371 (1996) 116.

[19] D. moermann et al.: on the efficient operation of a CsI-coated GEM photon detector. Nucl. Intr. And meth A471(2001)333.

[20] F. Sauli.: Principles of operation of multiwire proportional and drift chambers, CERN 77-09.

[21] C.M.B. Monteiro et al.: A curved-grid gas proportional scintillation counter instrumented with a 25-mm active-diameter photosensor., Nucl. Instrum. And Meth. A522 (2004) 407.

[22] A. Oed et al.: Micro pattern structures for gas detectors. Nucl. Instr. And Methods A471 (2001)109.

[23] A. Breskin.: The multi-step avalanche chamber, a new concept in fast high rate particle detectors. Nucl. Instrum. Methods 161, 19 (1979).

[24] Carola Richter et al.: On the efficient electron transfer through GEM. Nucl. Instr. And Meth. A478 (2002) 528

[25] A. Buzulutskov et al.: Further studies of the GEM photomultiplier. Nucl. Instrum. and Meth. A442 (2000) 68

[26] G.P. Guedes et al.: Two-dimensional GEM imaging detector with delay-line readout., Nucl. Instrum. and Meth. A513 (2003) 473.

[27] V. Dangendorf et al.: Time-resolved fast neutron imaging: simulation detector performance submitted to Nucl. Intr. And Meth A535(2004)93.

[28] J. Veloso et al., Rev. Sci. Instrum. 71(2000)2371.

[29] J.M. Maia et al.: Avalanche-ion back-flow reduction in gaseous electron multipliers based on GEM/MHSP., Nucl. Instr. and Meth. A523(2004)334.

[30] MAXWELL 3D, ANSOFT Co. Pittsburg, PA, USA.

[31] GARFIELD by R.Veenhof, Nucl. Instr. and Meth. A419(1998)726, Version 6.33, Nov. 1999

[32] Print electronics, IQS Biometric Solutions P.O. Box 2109, 27120 Kiryat Byalik Israel

[33] D. Mörmann et al. : Operation principles and properties of the multi-GEM gaseous photomultiplier with Ref photocathode., Nucl. Instr. and Meth. A530(2004)258.

[34] Z. Fraenkel et al. : "A hadron blind detector for PHENIX experiment at RHIC", submitted to Nucl. Instr. and Meth., Eprint version : http://xxx.lanl.gov/abs/physics/0502008A.

[35] Buzulutskov et al.: The GEM photomultiplier operated with noble gas mixtures., Nucl. Instr. and Meth. A443 (2000) 164.],

[36] A. Breskin, at al., GEM photomultiplier operation in CF4, Nucl. Intr. And Meth A 483 (2002) 670.

[37] F. Sauli website: http://gdd.web.cern.ch/GDD/

[38] A. Breskin et al.: New approaches to spectroscopy and imaging of ultrasoft-to-hard X-rays, Nucl. Intr. And meth A310 (1991) 57

[39] A. Breskin.: Secondary emission gaseous detectors: a new class of radiation imaging detectors. Nuclear Physics B (Proc. Supp.) 44 (1995) 351.

[40] V. Dangendorf et al.: Detectors for time-of-flight fast-neutron radiography 1.Neutron-counting gas detector., (physics/0408074).

[41] A. Di Mauro et al.: Photoelectron backscattering effects in photoemission from CsI into gas media., Nucl. Instr. and Meth. A371 (1996) 137.

[42] A. V. Lyashenko1 et al.: Advances in Ion back-flow reduction in cascaded MHSP/GEM electron multipliers., in progress.

[43] BSF, project number 2002240, Weizmann Institute of Science number 3171.

[44] G. Garty et al.: The performance of a novel ion-counting nanodosimetery., Nucl. Instr. and Meth. A492(2002)212.

[45] V. Dangendorf et al.: Nutrons detection using the thick gas electron multiplier. , in progress.

[46] A. Breskin et al.: Ion induced effects in GEM and GEM/MHSP gasous photomultiplier for the UV and visible spectral range., Physics/0408076.